Published online 28 April 2012

Nucleic Acids Research, 2012, Vol. 40, No. 15 ***e113***
doi:10.1093/nar/gks334

A new way of measuring apoptosis by absolute quantitation of inter-nucleosomally fragmented genomic DNA

David J. Hooker[1,*], Masqura Mobarok[1], Jenny L. Anderson[1,2], Reena Rajasuriar[3,4], Lachlan R. Gray[1,5], Anne M. Ellett[1], Sharon R. Lewin[1,3,6], Paul R. Gorry[1,3,7] and Catherine L. Cherry[1,3,6]

[1]Centre for Virology, Burnet Institute, 85 Commercial Road, Melbourne, Victoria 3004, Australia, [2]Department of Microbiology, [3]Faculty of Medicine, Nursing and Health Sciences, Monash University, Clayton, Victoria 3168, Australia, [4]Faculty of Medicine, University Malaya, Kuala Lumpur, Malaysia, [5]Department of Biochemistry and Molecular Biology, Monash University, Clayton, [6]Infectious Diseases Unit, The Alfred Hospital, Melbourne and [7]Department of Microbiology and Immunology, The University of Melbourne, Parkville, Victoria 3010, Australia

Received December 20, 2011; Accepted April 2, 2012

ABSTRACT

Several critical events of apoptosis occur in the cell nucleus, including inter-nucleosomal DNA fragmentation (apoptotic DNA) and eventual chromatin condensation. The generation of apoptotic DNA has become a biochemical hallmark of apoptosis because it is a late 'point of no return' step in both the extrinsic (cell-death receptor) and intrinsic (mitochondrial) apoptotic pathways. Despite investigators observing apoptotic DNA and understanding its decisive role as a marker of apoptosis for over 20 years, measuring it has proved elusive. We have integrated ligation-mediated PCR and qPCR to design a new way of measuring apoptosis, termed ApoqPCR, which generates an absolute value for the amount (picogram) of apoptotic DNA per cell population. ApoqPCR's advances over current methods include a 1000-fold linear dynamic range yet sensitivity to distinguish subtle low-level changes, measurement with a 3- to 4-log improvement in sample economy, and capacity for archival or longitudinal studies combined with high-throughput capability. We demonstrate ApoqPCR's utility in both *in vitro* and *in vivo* contexts. Considering the fundamental role apoptosis has in vertebrate and invertebrate health, growth and disease, the reliable measurement of apoptotic nucleic acid by ApoqPCR will be of value in cell biology studies in basic and applied science.

INTRODUCTION

Apoptosis is a fundamental, conserved and carefully orchestrated cell-death process that is critical for vertebrate and invertebrate embryogenesis, tissue homeostasis and normal aging (1). The fine control of apoptosis can be dysregulated *in vivo* by disease (2–5), intentionally or unintentionally by therapy (6–9) and *in vitro* by stress signals such as heat, chemical agents, UV- and γ-irradiation (10). Understandably, measuring apoptosis is an important objective in many fields of pure and applied research.

Molecular events within an apoptotic cell follow two key pathways: the extrinsic pathway that begins at the cell membrane with the binding of cytokine ligands to tumour necrosis factor alpha (TNFα) family death receptors, or the intrinsic pathway initiated at the mitochondrial membrane. There is thought to be significant interplay between the two pathways (10), and further downstream both pathways merge in the activation of cysteinyl, aspartate-specific proteases -3 and 6 (caspase-3 and -6). Cleavage of the enzyme DNA fragmentation factor 45 (DFF45) to the active 40-kDa form by active caspase-3 causes endonucleotyic breakage of chromatin and eventual chromatin condensation, one of the classic morphological features of cell apoptosis (11,12).

Fortunately, the molecular events of apoptosis now understood have allowed the development of methods to monitor—whether as detection or as measurement—various markers of apoptosis, for example, the degree of caspase-3 activation, cell membrane asymmetry of phophatidylserine, shifts in mitochondrial membrane potential, or detection of intact and cleaved poly-ADP-ribose-polymerase that binds at DNA strand breaks.

*To whom correspondence should be addressed. Tel: +61 3 85062315, +61 4 14539729; Fax: +61 3 92822100; Email: dahoo@burnet.edu.au

© The Author(s) 2012. Published by Oxford University Press.
This is an Open Access article distributed under the terms of the Creative Commons Attribution Non-Commercial License (http://creativecommons.org/licenses/by-nc/3.0), which permits unrestricted non-commercial use, distribution, and reproduction in any medium, provided the original work is properly cited.

However, methods to assess apoptotic markers can have numerous limitations; examples include a qualitative or comparative ability to measure, a lack of sensitivity especially to measure changes at low levels, a requirement for live cells at the time of measurement (and therefore limited utility in longitudinal studies), a restricted and non-linear dynamic range and low throughput.

Within the classic chromatin condensation phase of apoptosis is a terminal molecular stage, that of inter-nucleosomal fragmentation of genomic DNA (apoptotic DNA). Apoptotic DNA is a particularly valuable marker to measure for two reasons: (i) it is considered a biochemical 'hallmark' because it is a late 'point of no return' step in both the extrinsic and intrinsic pathways (10,13–15) and (ii) the stability of double-stranded apoptotic DNA gives greater utility than methodologies that rely on unstable cell lysates or live cells at the point of measurement. Apoptotic DNA fragmentation is inducible in cell culture then detectable by electrophoretic separation of oligo-nucleosomal-sized nucleic acid populations, seen as a ladder of multiples of 180–200 bp. However, DNA fragmentation from a biological specimen is typically too low to be electrophoretically visualized even though changes at these low levels can reflect significant shifts from cell equilibrium (16). Despite detection of amplified apoptotic fragments from vertebrate and invertebrate tissues in 1997 (17) there is currently no robust method for *measuring* in absolute terms the amount of apoptotic nucleic acid from cells, and hence no method for using this value as a sensitive and important marker for the extent of apoptosis.

In this report we integrate ligation-mediated PCR with qPCR to measure in absolute terms the amount of apoptotic nucleic acid from cells. Termed ApoqPCR, we show this method to be reliable, to have wide dynamic range, to have the required sensitivity for distinguishing low yet biologically relevant levels of apoptosis, to not require live cells at the point of measurement, and to be able to work from minute tissue samples, thus overcoming or improving significantly upon the limitations of other current methods. We demonstrate the utility of ApoqPCR in an *in vitro* context using samples equivalent to 100 cells or less, and in an *in vivo* context by investigating the dysregulation of apoptosis by virus (HIV-1) using long-term archived biological samples.

MATERIALS AND METHODS

Cells and genomic DNA

Peripheral blood mononuclear cells (PBMC) were collected with approval by the local Human Research and Ethics Committee and written, informed consent from all subjects. PBMC were purified by Ficoll density gradient centrifugation and phosphate-buffered saline (PBS, pH 7.2, $CaCl_2$ and $MgCl_2$-negative; Gibco) washes, then suspended in PBS and snap-frozen at −80°C.

PBMC used in ApoqPCR validation experiments were purified from HIV-seronegative buffy coat by Ficoll density gradient centrifugation, cultured at 2×10^6 cells/ml and phytohaemagglutinin-stimulated for 48 h in RPMI 1640, supplemented with 10% foetal bovine serum (batch tested for PBMC growth; Invitrogen), 1 U/ml penicillin and streptomycin, 2 mM L-glutamine and 20 U/ml interleukin-2. Jurkat cells for validation experiments and completely apoptotic DNA were grown to log phase at 1×10^6 cells/ml in RPMI 1640 with serum, antibiotics and glutamine as above (RF-10). Genomic DNA (gDNA) was purified with QIAamp DNA mini-columns (Qiagen, Hilden, Germany; columns designed for purification of nucleic acid of sizes <200 bp to >50 kbp), eluted and diluted in 10 mM Tris–HCl pH 8.5 at 25°C, 0.5 mM EDTA, quantified spectrophotometrically and stored at −80°C.

Generation and verification of completely apoptotic DNA

Fifteen millilitre of log-phase Jurkat cells were pelleted, re-suspended in fresh RF-10 at 37°C to 10^6 cells/ml then incubated at 37°C/5 h with or without 8 μM staurosporine (Sigma-Aldrich, Sydney, Australia). For each, gDNA was column-purified from 1.5 ml and compared by agarose gel electrophoresis with trace analysis (see Supplementary Methods section). Additionally for each, 6 ml cells were collected, washed and re-suspended in PBS to 2×10^7 cells/ml for triplicate 100 μl cells per microwell. TUNEL procedure for cell suspensions followed the *In Situ* Cell Death Detection Kit, Fluorescein (Roche, Mannheim, Germany) with the following modifications: after pelleting cells, supernatant was aspirated and cells gently re-suspended in 100 μl/well of fixation/permeabilization solution (Cytofix/Cytoperm kit, BD Biosciences/Pharmingen, CA, USA). After incubation for 20 min at 4°C, cells were washed at this and subsequent wash stages two times at RT with Perm/Wash buffer (Cytofix/Cytoperm kit). After final washes cells were re-suspended in 250 μl/well 1% paraformaldehyde (EM grade, Polysciences, Warrington, PA, USA) in PBS, stored 4°C in the dark for up to 16 h and analysed by flow cytometry at excitation 488 nm, detection 530 nm using a BD FACScan (BD Biosciences).

Construction of apoptotic standard DNA dilutions

The concentration of Jurkat cell completely ('100%') apoptotic DNA was determined spectrophotometrically and made to 23.15 ng/μl. Six serial 4-fold dilutions were then made from 9.26 ng/μl (40%) to 9.04 pg/μl. Single-use aliquots of these standards were stored at −80°C prior to use.

ApoqPCR

Ligation-mediated PCR (17,18) was significantly modified here for ApoqPCR. Annealing/ligation reactions comprised 17.28 μl standard DNA (at 9.26 ng/μl to 9.04 pg/μl), or test sample gDNA (x ng/μl to 200 ng maximum), or a no-template control (NTC, PCR grade water), 0.96 μl each of oligonucleotides 24-mer DHApo1 and 12-mer DHApo2 (Sigma-Aldrich, Sydney Australia) (both at stock 0.005 nmol/μl in 10 mM Tris–HCl pH 8.5 at 25°C, 0.5 mM EDTA) and 4.8 μl of 5× ligation buffer containing polyethylene glycol (Invitrogen), to make a final volume of 24 μl. The sequences of DHApo1 and DHApo2 respectively are, 5′ to 3′: AGCACTCTCGAGCCTCTCACCGCA and T GCGGTGAGAGG (17). Oligonucleotides were annealed to form blunt-ended partially double-stranded linkers by stepwise cooling from 55°C to 15°C in 5°C/8 min increments

then 10°C/20 min employing a thermal cycler. At the 10 min point of 10°C the program was paused and 2.4 U T4 DNA ligase (Invitrogen, diluted from 5 U/μl to 1 U/μl in PCR grade water) was added, mixed and the temperature continued for 10°C/10 min then ramped to 16°C/16 h for ligation. Post-ligation reactions were diluted to 80 μl in 10 mM Tris–HCl pH 8.5 at 25°C, 0.5 mM EDTA and 7.5 μl used in each of triplicate 25 μl qLM–PCR reactions. Thus for the six 4-fold diluted standards, qLM–PCR reactions contained 15 000 pg down to 14.6 pg of completely apoptotic DNA. Twenty-five microlitres of qLM–PCR reactions contained 7.5 μl diluted annealing/ligation reaction, 0.63 μl additional 50 pmol/μl 24-mer, and final concentrations of 1× Taq DNA polymerase buffer (Fisher Biotech, Wembley, Western Australia), 320 μM (each) dATP, dTTP, dGTP, dCTP (Promega), 2 mM $MgCl_2$, 0.4× SYBR Green I (Invitrogen), PCR grade water and 0.1 U/μl Taq DNA polymerase (Fisher Biotech or Scientifix, Cheltenham, Victoria, Australia) as a Taq DNA polymerase–antibody complex allowing a PCR hot-start. The Taq DNA polymerase–antibody complex was prepared with 'Jumpstart' Taq DNA polymerase antibody (Sigma-Aldrich, Missouri, USA) according to instructions. Cycling conditions were as follows: Employing a Stratagene MX3000P instrument (Agilent Technologies, Stratagene, La Jolla, CA, USA) with software MXPro version 4.10, qLM–PCR reactions were heated to 94°C for 1 min to activate Taq DNA polymerase and release 12-mers, then ramped to 72°C for 4 min to re-anneal the target DNA and generate complementary sequence to the ligated 24-mers. PCR then proceeded over 40 cycles of 94°C for 1 min followed by annealing/extension at 72°C for 3 min. Fluorescence data was collected at the end of annealing/extension steps.

Standards to estimate cell number equivalence of gDNA were also constructed. PBMC from ~100 ml blood were isolated by Ficoll density gradient centrifugation, washed 5× with room temperature PBS to remove platelets, re-suspended in 1 ml PBS, accurately counted by haemocytometer (mean of four counts), and re-suspended to 6×10^7 cells/ml in freshly prepared lysis buffer (10 mM Tris–HCl pH 8.0 at 25°C, 1 mM EDTA, PCR grade water; final concentrations of 0.002% Triton X-100, 0.002% SDS and 0.8 mg/ml proteinase K added just before use). Cells were lysed at 56°C for 1–2 h with occasional agitation, then proteinase K inactivated at 95°C for 15 min. Similar protocols are routinely performed in qPCR laboratories (19–21). Standards were created as six 5-fold dilutions from 50 000 cells worth/1.62 μl to 16 cells worth/1.62 μl, divided into single-use aliquots and stored at −80°C prior to use.

Cell Number qPCR consisted of triplicate 25 μl reactions each containing 1.62 μl of standard DNA cell lysate dilutions, or the same test sample gDNA used for the qLM–PCR reaction, or NTC, and final concentrations of 200 nM each of LK46 and LK47 primers (Sigma-Aldrich), 1× Brilliant II qPCR Master Mix (Agilent Technologies Stratagene, Forest Hill, Victoria, Australia) and PCR grade water. LK46 and LK47 primers span a 239-bp region of the single copy human CCR5 gene (22). Respective LK46 and LK47 sequences are, 5′ to 3′: GCT GTGTTTGCGTCTCTCCCAGGA and CTCACAGCCC TGTGCCTCTTCTTC. Adding 1.62 μl of test sample gDNA ensures that the same amount of gDNA is added to both qLM–PCR and Cell Number qPCR reactions. Cycling conditions were as follows (MX3000P): 95°C for 10 min to activate DNA polymerase followed by 40 cycles of 94°C for 20 s, 58°C for 30 s and 72°C for 30 s. Fluorescence data was collected at the end of annealing steps. Dissociation curves established that a single dominant product was synthesized for all standard dilutions, confirmed by electrophoretic examination. For both qLM–PCR and Cell Number qPCR, runs were not accepted if the standard curve correlation was less than $R^2 = 0.985$. Final C_t's from triplicates of standards and samples were not accepted if the C_t range of triplicates spanned ≥0.8.

Comparison and validation of ApoqPCR against other apoptosis quantifiers

In parallel, log-phase Jurkat cells at 10^6/ml were incubated with 0, 2 or 20 μM camptothecin (Sigma-Aldrich) or vehicle (0.4% DMSO, simulating DMSO with 20 μM camptothecin) with cells removed and processed at 0, 1, 2, 3, 4 and 5 h. Three experiments for apoptosis measurement were then performed on the one cell pool at each time-point:

Terminal deoxynucleotidyl transferase-mediated dUTP nick end labelling with measurement by flow cytometry (TUNEL/FACS)

At each time-point 7 ml cells were pelleted, washed and re-suspended in PBS to 2×10^7 cells/ml for quadruplicate 50 μl cells per microwell. TUNEL procedure for cell suspensions and flow cytometry was as described in 'Materials and Methods' section.

Active caspase-3 measurement by ELISA

For each time-point 6 ml cells were pelleted, washed, re-suspended and solubilized in 800 μl cell lysis buffer (BD Pharmingen) and stored at −80°C. Additional aliquots of lysate were also stored at −80°C for protein estimation (in duplicate) using the Bio-Rad DC protein assay (Bio-Rad Laboratories). Optical density measurements were confirmed in the linear range by performing duplicate reactions of three dilutions of lysate for each time-point. The ELISA followed BD Pharmingen's procedure in the 'human active caspase-3 ELISA pair technical data sheet'. The working dilution of horseradish peroxidase antibody was 1 in 2500. Three ELISAs were performed at separate times using duplicate 100 μl lysate samples for each ELISA, and optical densities measured with a Thermo Multiskan Ascent plate reader (Electron Corporation). Final optical density figures were obtained by first correcting $OD_{450\ nm}$ by subtracting $OD_{570\ nm}$ for all wells including blank (assay diluent), then subtracting corrected blank from corrected test samples.

ApoqPCR

One millilitre of cells at each time-point was pelleted, washed and re-suspended in 200 μl PBS and stored at −80°C. Genomic DNA was then purified and subjected to ApoqPCR.

Capability of ApoqPCR to measure small changes in apoptosis

In a different series of three separate experiments examining ApoqPCR's sensitivity at low (more biologically relevant) apoptosis levels, PHA/IL-2 stimulated PBMC were exposed at 1×10^6 /ml for 3.5 h to 12 camptothecin concentrations from 0 to 0.2 μM in 0.02 μM increments and a strong positive 2.0 μM control, or to concentrations from 0 to 0.3 μM in 0.03 μM increments +3.0 μM. Three experiments for apoptosis measurement were then performed for each camptothecin dose:

TUNEL/FACS

For each camptothecin dose 6 ml cells were collected, washed twice with PBS and re-suspended in [PBS + 1% foetal bovine serum] to 2×10^7 cells/ml for triplicate 100 μl cells per microwell. TUNEL procedure for cell suspensions and flow cytometry was as described in 'Materials and Methods' section.

Phycoerythrin-tagged Annexin V + 7-AAD with measurement by flow cytometry (PE-Annexin-V/FACS)

Cells were processed and flow cytometry performed as recommended (PE-Annexin V apoptosis detection kit I, BD Biosciences). Controls included cells exposed to 0, 0.20, 0.30 and 2 or 3 μM camptothecin, either unstained, stained with PE-Annexin V without 7-AAD or stained with 7-AAD without PE-Annexin V. Specific PE-Annexin V-positive cells (necrosis-negative) were measured with post-acquisition compensation (FlowJo 7.6.1).

ApoqPCR

Genomic DNA purification and ApoqPCR was performed as for validation in Jurkat cells (above).

ApoqPCR utility with minute samples: comparison of apoptosis measurement with either ApoqPCR or fluorescence microscopy using sub-100 cell-equivalent sample sizes

For each of three independent experiments, log phase Jurkat cells at 1×10^6 cells/ml in pre-warmed RF-10 were exposed to either 0, 0.2, 0.4 or 0.8 μM staurosporine for 3 h at 37°C. Samples were divided and prepared for apoptosis measurement by either ApoqPCR or fluorescence microscopy:

Fluorescence microscopy

Two ml of cells were pelleted, washed and re-suspended in PBS to 3×10^6 cells/ml. Forty microlitres of these cells were settled by gravity for 30 min at 37°C onto #1.5 glass coverslips (Menzel-Glaser, Germany) pre-coated with 0.01% poly-L-lysine in wells of a 24-well plate. After cell adhesion, excess liquid was removed and cells fixed at RT for 60 min in 3.7% paraformaldehyde (EM grade, Polysciences) in PBS. Cells were permeabilized on ice for 2 min in 0.1% Triton X-100 diluted in 0.1% tri-sodium citrate. After three washes with PBS, cells were stained with TUNEL reaction mixture (*in situ* cell-death detection kit, fluorescein; Roche) at 37°C for 60 min, humidified in the dark. Cells were washed three times in PBS and co-stained for 20 min at RT in the dark in PBS containing 1.0 U/ml Texas Red-conjugated phalloidin (Molecular Probes) to detect actin and 2.5 μg/ml Hoechst 33258 (Molecular Probes) to detect nuclei. Controls included 0.8 μM staurosporine-exposed cells then treated with (i) TUNEL label solution only (no phalloidin, no Hoechst) to register background from unincorporated FITC–dUTP, (ii) PBS as autofluorescence control (no phalloidin, no Hoechst), (iii) TUNEL reaction mixture (label+enzyme, no phalloidin, no Hoechst) and (iv) PBS (with phalloidin and Hoechst). Cells were washed three times in PBS then mounted onto glass slides with aqueous Gel Mount (Sigma) and air dried for 2 h. Mounted coverslips were imaged in *z*-series using a 40× objective lens (0.65–1.35 NA) and a CoolSNAP HQ camera (Photometrics) fitted on a DeltaVision RT fluorescence imaging system (Applied Precision). Samples were blinded prior to imaging and, for each sample, 20 randomly selected fields were imaged. Out-of-focus light was digitally removed from images using the associated softWoRx deconvolution software (Applied Precision). Images were viewed using softWoRx Suite Version 1.2 software, adjusted to identical display values and image files saved. Image files were blinded and manually counted for TUNEL-positive and total whole cells. TUNEL-positive cells were expressed as a percentage of total whole cells per field. The number of cells per field was routinely less than 100. Though TUNEL-positive cells varied in their TUNEL fluorescence intensity correlating with the staurosporine concentration, even very weak TUNEL-positive cells were clearly distinguishable from negative cells and thus counted as positive. See Supplementary Figure S6. Representative images from one experiment are shown. Data was combined from the three independent experiments for analysis.

ApoqPCR

ApoqPCR was performed on gDNA from 1.2 ml of cells as described previously. Cell Number qPCR served to determine gDNA concentration that represented sub-100 cell levels. Diluted DNA at 47 pg/μl was added to annealing/ligation reactions. For each experiment values were obtained from six individual replicate wells for qLM–PCR and for Cell Number qPCR.

Statistical analyses

All statistical analyses were undertaken using Stata 10.1 (StataCorp, College Station, TX, USA). The tests used for each data set are described in the text.

RESULTS

ApoqPCR was designed as two stages. The first stage incorporated annealing/ligation reactions with ligation-mediated PCR (Figure 1) in real-time ('qLM–PCR'); threshold cycles generated by gDNA from test samples were referenced against an apoptotic DNA standard curve to determine the amount (picogram) of apoptotic DNA. The apoptotic DNA standard curve was constructed by plotting threshold cycles against serially diluted

amounts of completely apoptotic DNA (see below). In different qPCR reactions, the second stage measured cell number of test samples from the same amount of gDNA as in qLM–PCR reactions ('Cell Number qPCR'), referenced against a second, Cell Number, standard curve.

Generation and verification of completely apoptotic DNA

In order to construct an apoptotic DNA standard curve, completely apoptotic DNA was generated, defined as the absence of any typically high molecular weight gDNA and complete conversion into apoptotic fragments as determined by post-electrophoretic quantification of gel track trace intensity. The conservation of apoptosis across cells, tissues and organisms (17) enabled the valid use of cultured Jurkat cells as a source. Jurkat cells also conveniently enabled the production of large quantities of gDNA if necessary. Incubation of Jurkat cells with 1, 2 and 4 μM staurosporine for 5 h generated fragmented DNA populations with a range of unconverted high molecular weight gDNA from 6.1% to 1.8% as determined by trace quantification (Supplementary Figure S1a and S1b and Supplementary Methods section). Optimally, incubation for 5 h at 37°C/5% CO_2 with 8 μM staurosporine generated fragmented DNA with effectively 0% unconverted gDNA (Figure 2a and b). Importantly, the relative size distribution of fragments generated by staurosporine was equivalent to the profile found naturally (Supplementary Figure S2a and S2b). To verify the definition of completely apoptotic DNA we measured apoptosis by another accepted quantifier, terminal deoxynucleotidyl transferase-mediated nick end labelling with dUTP–fluorescein (TUNEL), with TUNEL-positivity assessed by flow cytometry (FACS) from fractions of the same cells. Mean TUNEL-positivity was 99.3% (Figure 2c).

Reproducibility of completely apoptotic DNA from different source preparations

With completely apoptotic DNA acting as a core reagent it was necessary to establish reproducibility. Trace profiles from three separate experiments showed complete conversion to fragmented DNA (Supplementary Figure S3a and S3b) and was verified by a mean TUNEL-positivity of 99.0% (nine replicates over three experiments, range 98.6% to 99.5%) (Supplementary Figure S3c).

Completely apoptotic DNA from these three experiments was separately made the target DNA in qLM–PCR reactions to assess the consistency of standard curve threshold cycles (C_t's). For each preparation, reactions generated eight replicate C_t's with 15 000 pg of

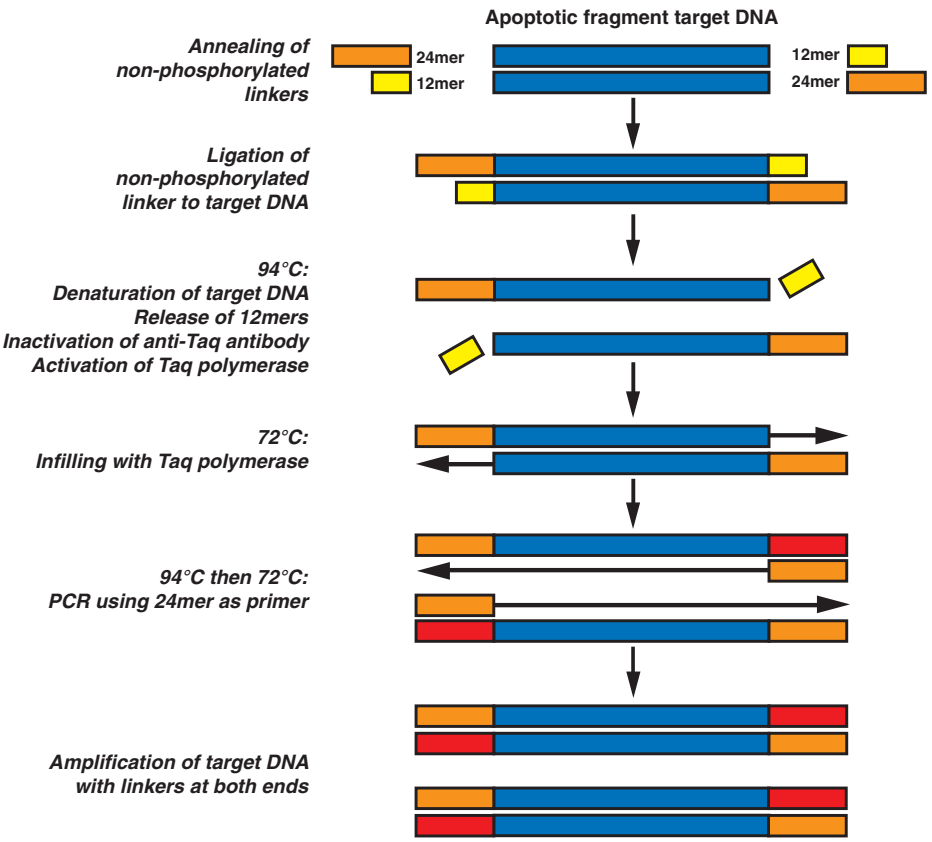

Figure 1. Molecular process of ligation-mediated PCR. Non-phosphorylated oligonucleotides are annealed then blunt-end ligated to target apoptotic DNA within the gDNA population. Heating to 94°C releases the unligated 12-mers and dissociates the monoclonal antibody from Taq polymerase, allowing synthesis at 72°C of the complement of the 24-mer sequence. Subsequent cycles at 94°C then 72°C allows amplification of target DNA using only the 24-mer as PCR primer. Blue boxes: single strands of target DNA; yellow boxes: 12-mers; orange and red boxes: 24-mers and their synthesized complement respectively. Process modified from Staley *et al.* (17).

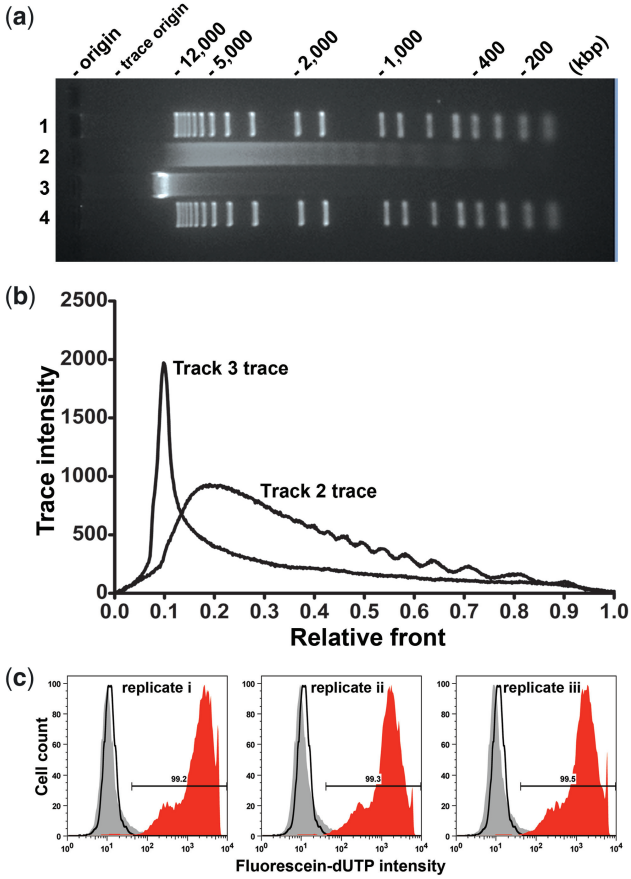

Figure 2. Production and verification of completely apoptotic DNA. (**a**) After 5 h incubation, Jurkat cell gDNA was purified as in 'Materials and Methods' section, electrophoresed together on a 1.5% agarose gel, stained with ethidium bromide then destained. Tracks 1 and 4: 500 ng per track molecular weight markers (1 kb Plus DNA ladder, Invitrogen). Track 2: 500 ng Jurkat gDNA incubated with 8 μM staurosporine for 5 h. Track 3:500 ng of untreated (staurosporine-negative) Jurkat gDNA. (**b**) Trace intensities of samples in tracks 2 and 3 from gel of (a). The location in the figure of the y-axis and the length of the x-axis are aligned with the gel in (a). The track 2 trace reveals a complete absence of high molecular weight (unfragmented) gDNA, hence defined as completely ('100%') apoptotic DNA. (**c**) The extent of apoptosis was verified by flow cytometric measurement of TUNEL-positivity of cells from the same experiment shown in (a) and (b). Gating excluded sub-cellular debris and selected the total cell population. At least 10 000 events were sorted at each measurement. Black line histogram: negative control cells after 5 h incubation (TUNEL label, no enzyme); autofluorescence controls showed peaks at equivalent positions to negative control (data not shown); grey tint histogram: three replicates of untreated cells after 5 h; red tint histogram: three replicates of cells treated with 8 μM staurosporine for 5 h. Mean TUNEL-positivity was 99.3%. To confirm reproducibility of generating completely apoptotic DNA, this experiment was repeated twice on separate occasions with comparable results (Supplementary Figure S3).

completely apoptotic DNA in qLM–PCR reactions (the upper limit of the standard curve), eight replicate C_t's with 234 pg (a mid range input amount) and eight replicate C_t's with 14.6 pg (the lower limit of the standard curve), covering a 1000-fold range of target DNA amount. Inter-preparation C_t variance was well within qPCR tolerances (Supplementary Figure S3d). Linear regression modelling confirmed that the input concentration of apoptotic DNA was the main predictor of C_t ($R^2 = 0.74$, $P < 0.0001$). Adding the source preparation of the apoptotic DNA into the model as a possible predictive variable did not improve the model (model $R^2 = 0.75$, $P < 0.0001$) nor was source preparation associated with C_t as an individual variable ($P > 0.6$). We conclude that the generation of completely apoptotic DNA is achievable, verifiable by another accepted quantifier, and reproducible.

Generation of an apoptotic DNA standard curve by integrating ligation-mediated PCR with qPCR

Completely apoptotic DNA was quantitated then diluted as six serial 4-fold dilutions covering a 1000-fold range of concentrations (15 000 to 14.64 pg of completely apoptotic target DNA in each qLM–PCR reaction). Robust reaction conditions newly developed for qPCR amplification were determined by systematic optimization of the following parameters: ligation conditions, standard curve range, type and concentration of fluorescent dye, replicate number, Taq DNA polymerase–antibody amount, linker manufacturer and purification, and linker concentration in annealing/ligation reaction. Figure 3a and b shows representative amplification plots (mean of triplicates) and standard curve. Electrophoresis of the standard curve products of qLM–PCR verified amplification of oligonucleosomal-sized apoptotic populations (Figure 3c). Electrophoresis of gDNA from numerous test samples and subjected to qLM–PCR also verified consistent amplification of apoptotic DNA (Supplementary Figure S4).

A lack of high molecular weight gDNA in apoptotic DNA standard curve reactions does not influence the threshold cycle value

The generation of completely apoptotic DNA meant that all standard curve C_t's are derived from reactions that do not contain high molecular weight gDNA (i.e. typically 35–50 kb after purification)—yet test samples, for example clinical sample gDNA, have sizes of 35–50 kb because only a minor fraction of input DNA is apoptotic. Therefore experiments were designed to determine whether or not the presence of high molecular DNA in standard curve reactions influences C_t. Our first approach was to generate zero-apoptotic gDNA by physical recovery of the 35–50 kb fraction after electrophoresis, then spiking that DNA into standard curve reactions. Unfortunately even as a control (zero-apoptotic DNA only), a significant C_t and apoptotic fragment amplification (visualized electrophoretically) was achieved indicating that complete physical separation of 35–50 kb DNA from lower molecular weight fragments was not possible. Our second approach was to mimic high molecular weight gDNA with the presence of 48.5 kb lambda (λ) phage gDNA in annealing/ligation reactions and hence in qLM–PCR reactions. Annealing/ligation reactions with high, medium and very low concentrations of target apoptotic DNA typically spanning the standard curve range of concentrations, and negative control (PCR-grade water), were spiked with or without a significant amount of λ DNA (New England Biolabs) at a quantity typical of biological sample gDNA (Supplementary Table S1). Raw C_t results showed no

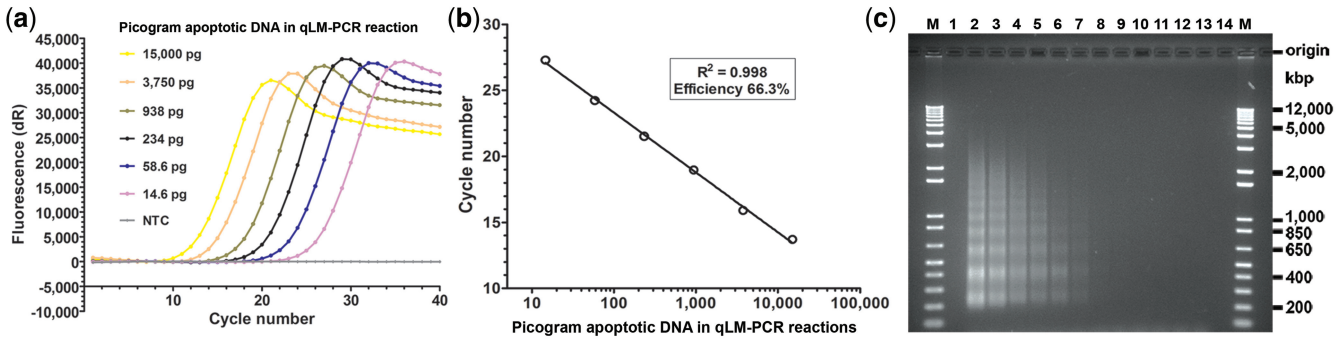

Figure 3. Merging ligation-mediated PCR with qPCR (qLM–PCR) to generate an apoptotic DNA standard curve. Apoptotic gDNA defined as complete was measured spectrophotometrically, diluted to cover a 1000-fold range of quantities and added to annealing/ligation reactions. Aliquots of diluted annealing/ligation reactions were added to qLM–PCR reactions and fluorescence of triplicates monitored in real time. (**a**) Mean of triplicate amplification plots shown. NTC: annealing/ligation with no gDNA into a qLM–PCR reaction as a no template control. (**b**) Representative standard curve showing correlation between C_t and amount of apoptotic DNA. Analysis of inter-run apoptotic standard curve consistency is reported in Supplementary Table S2a and S2b. (**c**) Electrophoresis on one agarose gel of actual qLM–PCR reactions (halted at cycle 20) using 2-fold dilutions of completely apoptotic DNA after ethidium bromide staining and de-staining. Fifty percent of each 25 µl reaction per well. M: 500 ng molecular weight markers per well with sizes shown on the right. Tracks 1 and 14: not loaded. Track 13: NTC. Track 2 to 12: 2-fold dilutions of complete apoptotic DNA from 15 000 pg to 14.6 pg in each qLM–PCR reaction. Gel shows that the qLM–PCR standard curve is generated by amplification of apoptotic fragments.

consistent effect on C_t by the presence of λ DNA and that in fact the C_t generated with λ DNA alone was equivalent to that generated by a target DNA amount ~1.3 logs lower than the least amount in the standard curve. The effect therefore lies beyond the lower limit of the standard curve. Linear regression modelling of the raw data revealed that the apoptotic DNA amount was strongly associated with C_t as expected ($P < 0.001$); however after correcting for apoptotic DNA amount, the presence or absence of λ DNA did not influence C_t ($P = 0.9$). We conclude from this that the absence of high molecular weight gDNA in standard curve reactions does not influence C_t.

Validation of ApoqPCR by comparison with other apoptosis quantifiers

ApoqPCR was validated first in camptothecin-exposed Jurkat cells by comparison against two other quantifiers, TUNEL/FACS with fluorescein–dUTP and active caspase-3 measurement by ELISA (Figure 4a, b and c). All three quantifiers exhibited sigmoidal profiles: an acceleration from 1 to 2 h, peaking at 2 to 4 h then slowing. Some contrasts are worth noting however: ApoqPCR values with camptothecin doses diminished beyond 4 h unlike TUNEL/FACS. ApoqPCR was more sensitive than TUNEL/FACS and caspase/ELISA at detecting and distinguishing apoptosis at lower levels: fold-differences relative to basal (0 µM) at 1 and 2 h respectively for ApoqPCR were 1.6 and 5.0 (with 2 µM), 2.8 and 9.3 (with 20 µM); for TUNEL/FACS were <1 and 2.7 (with 2 µM), <1 and 2.8 (with 20 µM); for caspase-3/ELISA were 1 and 3.9 (with 2 µM), 1 and 4.0 (with 20 µM). Moreover, the dynamic range of ApoqPCR allowed clearer resolution of values at higher levels of apoptosis: fold-differences relative to basal (0 µM) at 3 and 4 h respectively for ApoqPCR were 13.6 and 9.9 (with 2 µM), 26.4 and 20.2 (with 20 µM); for TUNEL/FACS were 6.6 and 6.7 (with 2 µM), 9.8 and 8.9 (with 20 µM); and for caspase-3/ELISA were 8.1 and 7.9 (with 2 µM), 9.7 and 9.1 (with 20 µM). For ApoqPCR the difference between 2 µM and 20 µM values reached significance at an earlier time point ($P = 0.0495$ from 1 h; Wilcoxon rank sum) compared to the other quantifiers. For TUNEL/FACS, the difference between 2 µM and 20 µM values did not reach significance until 3 h ($P = 0.100$ at 2 h, $P = 0.014$ at 3 h; Wilcoxon rank sum). The comparative values generated by caspase-3/ELISA with 2 µM and 20 µM doses were not different over the time course (best $P = 0.20$ at 5 h; Wilcoxon rank sum). This analysis suggests ApoqPCR to be more sensitive and to have a greater dynamic range than the other two quantifiers.

Secondly, ApoqPCR was compared against TUNEL/FACS and Annexin-V/FACS using PBMC. Here we were particularly interested to evaluate ApoqPCR's sensitivity to register differences in apoptosis at low levels, the rationale being that *in vivo* levels are rarely as high as is possible *in vitro* (as in Figure 4a for example). PBMC were cultured with incremental doses of camptothecin to mimic apoptosis levels <5-fold above basal (Supplementary Figure S5; Figure 4d, e and f). From Figure 4d, e and f we note the following: the fold difference registered by ApoqPCR from 0 to 0.20 µM doses was 5-fold compared to 2-fold for both TUNEL and Annexin-V/FACS. TUNEL/FACS did not achieve a steady incremental increase in fluorescein-dUTP positivity compared to ApoqPCR and Annexin V/FACS. By Wilcoxon rank sum ($n_1 = n_2 = 6$ at each comparison), ApoqPCR values were different comparing 0.04 to 0.10 µM doses, and 0.10 to 0.16 µM doses ($P = 0.002$ and 0.001 respectively). TUNEL/FACS values were not different comparing 0.04 to 0.10 µM ($P = 0.5$) but were different comparing 0.10 to 0.16 µM ($P = 0.021$). Annexin-V/FACS achieved differences for both comparisons ($P = 0.001$ for each). This analysis indicates ApoqPCR has the potential to register subtle low-level changes in apoptosis, a valuable asset for clinically-oriented (and other) studies.

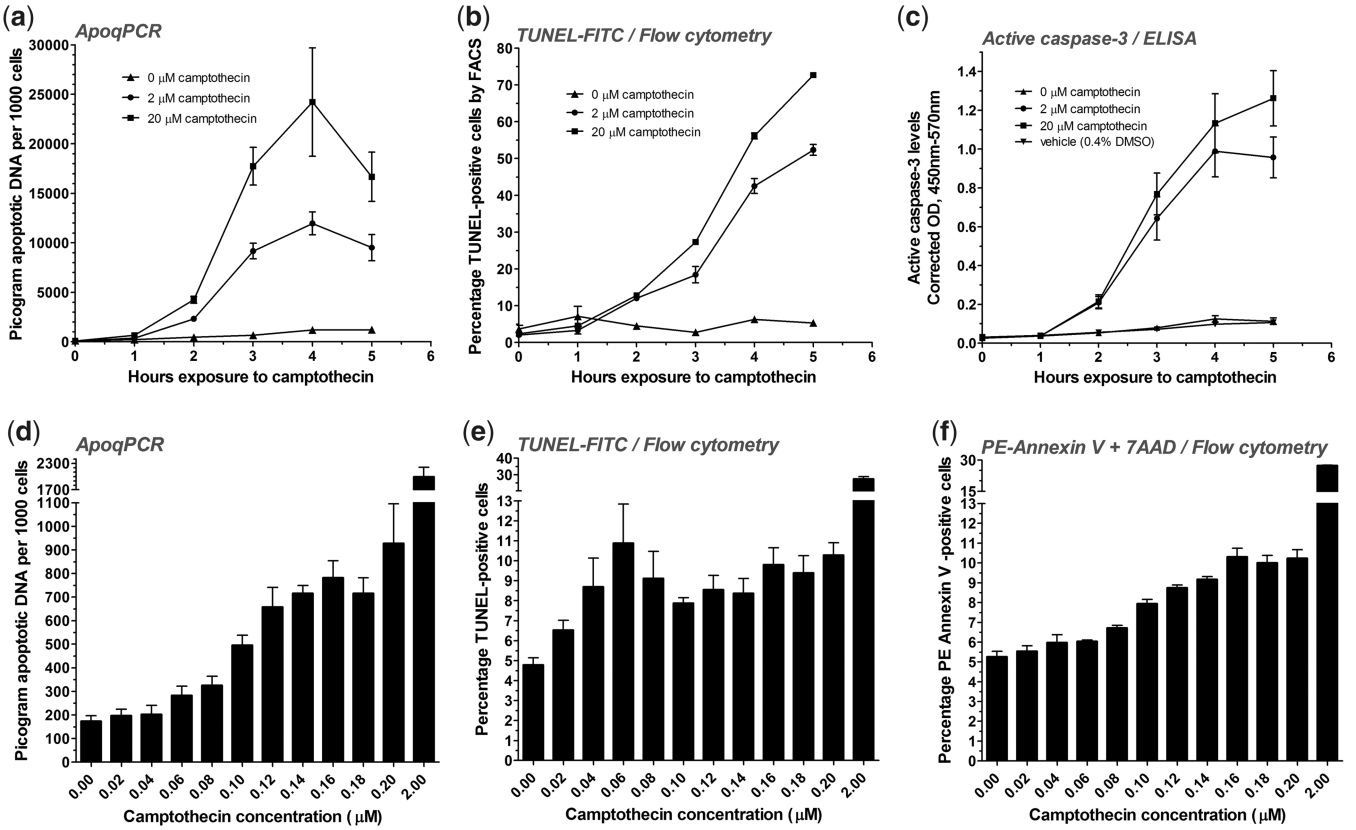

Figure 4. (**a–c**) Comparison and validation of ApoqPCR against other quantifiers of apoptosis. Log-phase Jurkat cells were incubated with 0, 2 or 20 μM of the topoisomerase I inhibitor camptothecin with cells removed and processed at 0, 1, 2, 3, 4 and 5 h. Apoptosis was measured on the one cell fraction at each time-point. Filled triangle, filled circle, filled square and filled inverted triangle define shifts in values due to 0, 2 and 20 μM camptothecin and vehicle respectively. Error bars ±1 SEM. (**a**) Changes in Jurkat cell apoptotic DNA levels over time as measured by ApoqPCR; 3 experiments where each experiment is a set of annealing/ligation reactions, qLM–PCR reactions and Cell Number qPCR reactions, generating nine replicates (see text). (**b**) Changes in Jurkat cell TUNEL-positivity with time as measured by flow cytometry; four measurements at each plotted value. At each measurement at least 10 000 events were sorted. (**c**) Changes in Jurkat cell active caspase-3 levels by ELISA; three independent experiments generating six replicates at each plotted value. (**d–f**) ApoqPCR exhibits competitive advantages in sensitivity when assessing low biologically relevant levels of apoptosis. In a separate series of independent experiments, changes in PBMC apoptotic DNA levels induced by small incremental increases in camptothecin dose were quantified in parallel by (**d**) ApoqPCR, (**e**) TUNEL/FACS and (**f**) Annexin V+7AAD/FACS. For each flow cytometry measurement at least 10 000 events were sorted. Bars ±1 SEM, $n = 6$ over two experiments; see also Supplementary Figure S5.

ApoqPCR characteristics: standard curve correlation and efficiency, replicate consistency, co-efficient of variation

Standard curve inter-run consistency established ApoqPCR as robust. Mean R^2 correlation for apoptotic DNA standard curves (qLM–PCR) was 0.993 ($n = 24$, range 0.986–0.999) and for Cell Number standard curves was 0.989 ($n = 24$, range 0.986–0.991) (Supplementary Table S2a, S2b and S2c). Efficiency of apoptotic DNA standard curves was consistent at ~70% probably due to the simultaneous amplification of multiple species of nucleic acid.

Replicate consistency (standard curve and test sample triplicates) was well within tolerances prescribed for real-time PCR: for qLM–PCR runs the mean C_t range within triplicate sets was 0.23 (range 0.00–0.66, $n = 150$ samples, 450 replicates); for Cell Number qPCR runs the mean C_t range within triplicate sets was 0.27 (range 0.02–0.97; $n = 150$ samples, 450 replicates).

We assessed ApoqPCR's co-efficient of variation (CV) using PBMC (see Supplementary Methods section). The mean CV due to variation in gDNA purification was 0.19 ($n = 5$, range 0.07–0.27), the mean inter-run CV was 0.21 ($n = 5$, range 0.14–0.26), and the mean intra-run CV was 0.11 ($n = 5$, range 0.04-0.14). These CV's compare favourably with other biological assays (23).

ApoqPCR utility: ApoqPCR can consistently measure apoptosis down to sub-100 cell-equivalent levels

To estimate the sensitivity of ApoqPCR to measure from minute input amounts, PBMC gDNA from four individuals and covering a range of apoptosis levels from very high to very low, were each diluted from 1 in 4 to 1 in 16 384 of their original concentration recovered by column purification. Each dilution was subjected to three ApoqPCR experiments comprising multiple annealing/ligations yielding 9 replicates for both qLM–PCR and Cell Number qPCR. Results show that ApoqPCR is able to provide consistent measurement down to the sub-100 cell-equivalent level and can quantitate from as little as

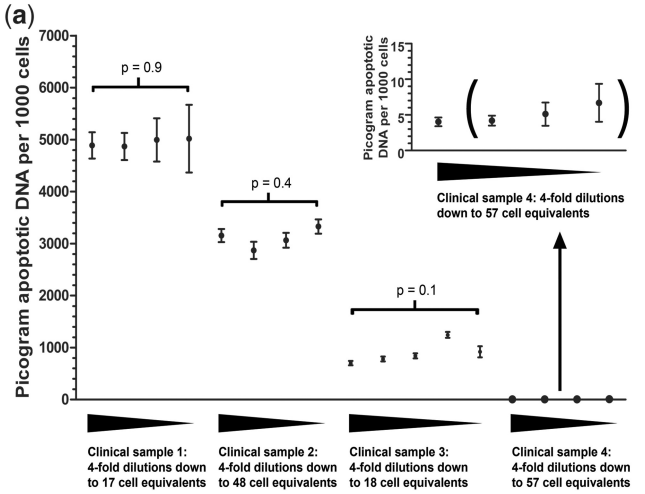

(b)

Staurosporine concentration	TUNEL-microscopy	TUNEL-microscopy	ApoqPCR	ApoqPCR
	Percent TUNEL-positive cells	Number of cells scored per field	pg apoptotic DNA per 1000 cells	Number of cells worth of gDNA used
	Mean	*Mean (Range)*	*Mean*	*Mean (Range)*
0 μM	1.35	89 (52 to 129)	224	45 (22 to 76)
0.2 μM	12.1	57 (19 to 104)	2,961	46 (34 to 58)
0.4 μM	30.7	60 (19 to 97)	5,814	47 (39 to 57)
0.8 μM	75.1	62 (23 to 111)	12,515	43 (26 to 62)

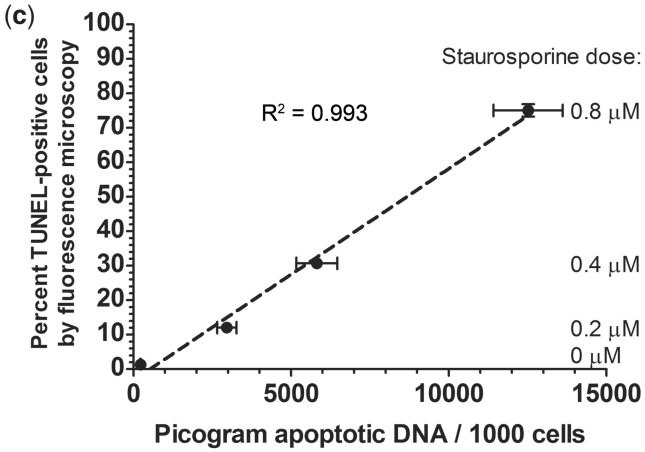

Figure 5. ApoqPCR utility in an *in vitro* context. (**a**) ApoqPCR can consistently measure apoptosis down to sub-100 cell-equivalent levels. Four-fold dilutions of PBMC gDNA from each of four individuals were constructed and pg apoptotic DNA/1000 cells determined in three experiments for all dilutions, yielding nine final values per dilution. Cell-equivalent values were determined by Cell Number qPCR. Error bars ± 1 SEM; *P*-values determined by Student's *t*-test comparing final values for the highest dilution against the lowest dilution. Final values are graphed when values determined by qLM–PCR or Cell Number qPCR arose within the limits of each of the two standard curves, with the exception of final (bracketed) values obtained for clinical sample 4, where, because of this sample's very low fragmentation level, qLM–PCR values arose below the standard curve despite reasonable cell numbers. This exception is shown to illustrate consistency at this very low apoptosis level (graph inset) and to indicate that it may be possible to extend the lower limits of the qLM–PCR standard curve. (**b**) and (**c**) Using Jurkat cells, ApoqPCR values are concordant with apoptosis- (TUNEL-) positive cells counted by fluorescence microscopy when working with minute samples (≤100 cell equivalents). Three independent experiments were combined. Table gives values obtained using either [mean cells counted per microscope field] or [mean cells worth of gDNA], each mean being <100. ApoqPCR achieves concordance with TUNEL-microscopy ($R^2 = 0.993$). Though ApoqPCR's standard errors are greater than those of TUNEL-microscopy in the graph, these SEM's are due to considerably lower number of replicates ($n = 18$ for ApoqPCR versus $n = 60$ for TUNEL-microscopy) and indicate that ApoqPCR can achieve concordant values with less replicates.

17 cells worth of gDNA (Figure 5a), providing a 3- to 4-log greater sample economy than current methods (Supplementary Table S3).

We further investigated ApoqPCR's utility to work with minute numbers of cells (≤100) by directly comparing apoptosis measured with ApoqPCR and with fluorescence microscopy. Apoptosis in staurosporine-exposed Jurkat cells was measured as percentage of TUNEL-positive cells in microscope fields with on average <100 cells per field, as compared to picogram apoptotic DNA per 1000 cells by ApoqPCR with <100 cells worth of gDNA. For ApoqPCR, the Cell Number qPCR arm served to inform the number of cells represented by the amount of gDNA added to qPCR reactions. For fluorescence microscopy, a large number of fields (60 fields over three independent experiments) were counted per dose and for controls, adding strength to the reference (TUNEL/microscopy) method and challenging ApoqPCR to meet it with fewer replicate measurements. Actin and nuclear staining helped distinguish debris and false-positives from true TUNEL-positive nuclei (Supplementary Figure S6). In Figure 5b and c, the straight line concordance ($R^2 = 0.993$) between the two methods reveals that values obtained by ApoqPCR increased in direct proportion with values obtained by TUNEL/microscopy. Both methods also exhibited proportional increase in apoptosis with staurosporine dose. Thus, the reliable measurement of apoptosis with low cell numbers illustrates the ability of ApoqPCR to provide a high level of sample economy and with more rapid throughput than fluorescence microscopy.

ApoqPCR utility: monitoring dysregulated apoptosis during viral infection

We tested ApoqPCR's ability to monitor apoptosis in an *in vivo* context. Dysregulated (elevated) apoptosis has been strongly implicated in HIV disease pathogenesis (24–26). We explored the clinical associations with PBMC apoptosis in well HIV patients by applying ApoqPCR to archived PBMC gDNA from an observational cohort of well-characterized patients who were studied 6 - monthly for up to 2 years (27) (Supplementary Table S4a and S4b). Paired PBMC samples were taken from 11 asymptomatic patients who underwent cohort visits while on no HIV therapy and during effective combination antiretroviral therapy (cART). In five cases, patients commenced cART on study and in six cases, patients who had undetectable viral loads on therapy took 'drug holidays' for personal reasons while on study. In all paired cases, PBMC apoptosis was lower while viral replication was suppressed by cART compared with levels seen in untreated HIV infection ($P < 0.001$, ANOVA), consistent with previous reports (28,29), but remained elevated

relative to levels seen in HIV-seronegative healthy controls ($P = 0.001$, ANOVA) (Figure 6a and b). Our cohort was not designed to assess the utility of PBMC apoptosis for *predicting* clinical outcomes in cART-treated HIV patients; nevertheless our results using ApoqPCR confirm HIV replication is an important effector of elevated PBMC apoptosis in clinically well patients.

DISCUSSION

The value of ApoqPCR depends on several premises being fulfilled concerning the core reagent, 'completely' apoptotic DNA: (i) that apoptotic fragmentation can essentially be complete in order to exploit spectrophotometric quantitation. Apoptosis inducers generate apoptotic nucleic acid fragments in a time and concentration-dependent manner; therefore we reasoned that complete fragmentation is possible. Trace quantification of electrophoresed DNA provided a sensitive way of measuring the extent of conversion, with further authentication by TUNEL/FACS. Other apoptosis inducers less potent than staurosporine may be unable to drive fragmentation to completion in a realistic time-frame considering the movement over time of some cells towards a necrotic phase; (ii) that the relative distribution of apoptotic fragment sizes generated by staurosporine is comparable to the profile generated *in vivo*. An inconsistency here would have introduced error into the comparison of test sample C_t's with standard curve C_t's because our qLM–PCR system is limited in its ability to amplify fragments $>\sim$2.5 kb; (iii) that the production of completely apoptotic DNA is reproducible from batch to batch. This is essential to achieve inter-laboratory consistency. However, completely apoptotic DNA production is very economical: 10 ml of staurosporine-exposed Jurkat cells is sufficient for 300 standard curves, for a maximum of 7500 test samples run in triplicate with those standard curves; (iv) that apoptotic fragments are authentically represented as blunt-ended and 5′-phosphorylated. Blunt-end predominance has previously been established using varying cell types and inducers (17,30), though to our knowledge it is unknown to what extent this occurrence is uniform. It is possible that some cell types, or apoptosis induced under certain conditions, may exhibit nucleic acid fragmentation with double-stranded ends that are not blunt, for example single-base overhangs. In these cases the design of ApoqPCR linkers could be modified to correctly ligate to cohesive ends. Interestingly, apoptotic inter-nucleosomal fragmentation also occurs in plants (31). ApoqPCR in its current form or with modified linkers could have utility in plant cell-death studies if plant inter-nucleosomal fragment termini can be characterized. A plant-specific core reagent of completely apoptotic DNA would be preferred in this case; (v) that high molecular weight gDNA in test samples does not influence the comparison of test sample versus standard curve C_t's. This was a consideration because standard curve C_t's are derived from reactions that *do not* contain high molecular weight gDNA (i.e. 35–50 kb after purification) yet test samples retain 35–50 kb sizes because only a minor fraction of input DNA is apoptotic.

In regard to the validation of ApoqPCR against other quantifiers, the 'sigmoidal' (acceleration/ plateau profile) over the time course in Jurkat cells (Figure 4a, b and c) has been observed by others (32–34) (BD Technical data sheet for human active caspase-3/ELISA pair). The similarities between markers measured by active caspase-3/ELISA and ApoqPCR reflects the relationship between activated caspase-3 levels and induction of DFF- 40/45, the endonuclease responsible for inter-nucleosomal cleavage of genomic DNA (12). We noted a contrast between TUNEL/FACS and ApoqPCR profiles in that ApoqPCR values diminished beyond the 4 h mark while TUNEL-positivity continued to rise. Here cell populations may be moving into a more necrotic phase with concomitant single-stranded non-apoptotic breaks, events that TUNEL registers (35–37). The diminishing values measured by ApoqPCR can therefore be attributed to this molecular tool's specificity for the classic double-stranded breaks of apoptotic cleavage.

(a)

Group		On cART		Not on cART	
		Range	Median	Range	Median
Patients commencing cART during study n = 5	Raw data: pg apoptotic DNA per 1000 cells	23 - 134	101	108 - 1160	446
	Log transformed data	1.37 – 2.13	2.00	2.03 – 3.06	2.65
Patients ceasing cART during study n = 6	Raw data: pg apoptotic DNA per 1000 cells	34 - 384	145	329 - 4354	773
	Log transformed data	1.53 – 2.58	2.16	2.52 – 3.64	2.89
Combined n = 11	Raw data: pg apoptotic DNA per 1000 cells	23 - 384	128	108 – 4354	760
	Log transformed data	1.37 – 2.58	2.11	2.03 – 3.64	2.88

(b)

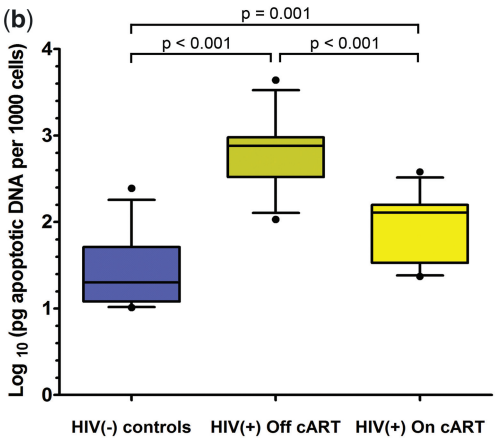

Figure 6. ApoqPCR utility in an *in vivo* setting. (**a**) and (**b**) In asymptomatic patients, PBMC apoptosis is lowered by effective combination antiretroviral therapy (cART) compared to levels during uncontrolled HIV replication, regardless of choice of cART regimen. Table outlines raw and log transformed data for 11 patients monitored over the period of either switching on or off cART, with transformed data presented graphically in (b) alongside data from 11 HIV-seronegative healthy controls. Outliers shown. Whiskers extend to the 10th and 90th percentiles; boxes, second and third quartiles round the median. The data analysis accommodated both the paired nature of results from HIV patients on and off cART and the independent nature of results from healthy controls by using a generalized estimating equations approach with a robust variance.

Diminishing values beyond the sigmoidal phase have been observed by others when assaying caspase-3 and -9 activity in staurosporine-treated Jurkat cells (33). In a different set of experiments, we assessed ApoqPCR's capacity to resolve low-level changes in PBMC apoptosis (Figure 4d, e and f), a more likely scenario in an (for example) *in vivo* context because subtle low-level changes in apoptosis can lead to shifts from homeostasis toward either tissue regression or unwanted growth (16). We found ApoqPCR met Annexin-V/FACS's sensitivity and exceeded that of TUNEL/FACS. When comparing data from the time course in Jurkat cells with the dose-responses in PBMC, we believe we have demonstrated that ApoqPCR has both broad dynamic range *and* sensitivity to distinguish subtle changes in apoptosis.

This methodology does have limitations. It will not give reliable results in samples where DNA integrity is compromised. Genomic DNA can be recovered from formalin fixed tissue though the average length of $<\sim$650 bp (38) precludes the use of ApoqPCR. Degraded forensic samples will also be unsuitable though in this context virtually all apoptosis measurement methods would be unreliable. Unlike flow cytometry, ApoqPCR cannot itself separate cell sub-populations; however measurement will be possible when sub-populations are first isolated by, for example, magnetic separation technology. Measurement from specific sub-populations may also be exploited by pairing laser-capture with our method in view of ApoqPCR's utility with small cell numbers ($\sim$500). A further limitation stems from the several forms of cell death being elucidated. As our understanding of the nuclear and cytoplasmic events of cell death continues to unfold, a more complex picture of programmed cell death is emerging with evidence that apoptosis is not the only type though it is a major one. Lysosomally-induced autophagic cell death (39), and some ischemic (40) and neurodegenerative (41) cell deaths have been reported, though the molecular events need further elucidation. Sperandio *et al.* (42,43) reported a programmed cell death ('paraptosis') with a distinct gene expression program from that of apoptosis and one that did not show evidence of inter-nucleosomal fragmentation and chromatin condensation. ApoqPCR will probably not have utility in these contexts; however it may find utility in clarifying the processing of chromatin in other programmed cell-death forms.

Several advances of ApoqPCR outline its versatility: (i) ApoqPCR overcomes the requirement for viable cells (as for flow cytometry) or fresh cell lysates (e.g. as for ELISA) at the point of measurement and in contrast works economically from an easily quantified, stable, readily stored and re-used form of one cell component—genomic DNA. An example here is the cohort used to study relationships between HIV infection, antiretroviral therapy and apoptosis. It is noteworthy that all PBMC samples used here had been archived for $>$5 years (some up to 11 years) by snap-freezing in PBS at -80°C before testing in parallel; hence results illustrate the potential of ApoqPCR to provide useful information in situations where most current methods (to our knowledge; i.e. those that require live cells or fresh lysates) would not be recommended. Significantly, ApoqPCR amplification of representative samples from those long-term stored samples used in Figure 6 is displayed in Supplementary Figure S4, showing that the integrity of the inter-nucleosomal DNA amplification is intact despite the fact that our storage conditions in this case could be considered less than optimal from a cell-survival point of view; (ii) genomic DNA is rapidly purified for PCR applications from many solid, suspension or cultured tissue types by column purification. Thus the 'starting material' is standardized, allowing straightforward comparative measurements from challenging tissues (e.g. solid tissues like spleen, liver, kidney) where other methodologies are not useful; (iii) having a standardized starting material also allows comparative apoptosis measurement across species and organism types because the challenges of multiple species-specific antibodies are avoided. Lastly (iv) ApoqPCR has capability to measure from minute tissue samples. In this report we investigated ApoqPCR's utility to measure apoptosis reliably with less than 100 cells worth of gDNA. If gDNA purification methods required only 100 cells or less, then ApoqPCR could achieve a dependable result; however this must be qualified by the fact that significant stochastic effects will be observed at this level, and, moreover, most purification methods require more cells. We see the main advantage as being one of sample economy, where precious samples can be diluted, aliquotted, and re-used again, perhaps in long-term studies. This part of the work does show however that ApoqPCR has the potential to achieve a result with 1 µl of blood ($\sim$1000 cells, some purification methods are designed for this amount) or with minute tissue amounts, for example punch needle skin biopsies. Additionally, in our estimation the throughput time is advanced by the 25% hands-on time of ApoqPCR compared to TUNEL-fluorescence microscopy.

In conclusion, we have employed apoptotic nucleic acid to design a new qPCR-based method for measuring the fundamental process of apoptosis, have validated this method against several current quantifiers, illustrated significant advantages of dynamic range, sensitivity and sample economy combined with throughput capability, and exemplified utility in *in vitro* and *in vivo* contexts. Considering the vital role apoptosis has in vertebrate and invertebrate health, growth and disease, the reliable measurement of apoptotic nucleic acid by ApoqPCR will be of value in cell biology studies in basic and applied science.

SUPPLEMENTARY DATA

Supplementary Data are available at NAR Online: Supplementary Tables 1, 2a–c, 3, 4a and b, Supplementary Figures 1–6 and Supplementary Methods.

ACKNOWLEDGEMENTS

D.J.H. thanks Assoc. Prof. Melissa Churchill and Assoc. Prof. Gilda Tachedjian for useful discussions, and to Maelenn Gouillou for assistance with statistical analysis. The authors gratefully acknowledge the contribution to

this work of the Victorian Operational Infrastructure Support Program received by the Burnet Institute.

FUNDING

The Australian Centre for HIV and Hepatitis Virology Research; Angior Foundation. National Health and Medical Research Council career development award (to C.L.C.). Funding for open access charge: The Burnet Institute.

Conflict of interest statement. D.J.H. states a conflict of interest: The Burnet Institute has filed a provisional patent on this technology. All other authors state there is no conflict of interest.

REFERENCES

1. Vaux,D.L. and Korsmeyer,S.J. (1999) Cell death in development. *Cell*, **96**, 245–254.
2. Thompson,C.B. (1995) Apoptosis in the pathogenesis and treatment of disease. *Science*, **267**, 1456–1462.
3. Burns,T.F. and El-Deiry,W. (2003) Cell death signalling in malignancy. *Cancer Treat Res.*, **115**, 319–343.
4. Green,D.R. and Evan,G.I. (2002) A matter of life and death. *Cancer Cell*, **1**, 19–30.
5. Hetts,S.W. (1998) To die or not to die: an overview of apoptosis and its role in disease. *JAMA*, **279**, 300–307.
6. Sheikh,M.S. and Huang,Y. (2004) Death receptors as targets of cancer therapeutics. *Curr. Cancer Drug Targets*, **4**, 97–104.
7. Sen,S. and D'Incalci,M. (1992) Apoptosis. Biochemical events and relevance to cancer chemotherapy. *FEBS Lett.*, **307**, 122–127.
8. Cherry,C.L., Lal,L., Thompson,K.A., McLean,C.A., Ross,L.L., Hernandez,J., Wesselingh,S.L. and McComsey,G. (2005) Increased adipocyte apoptosis in lipoatrophy improves within 48 weeks of switching patient therapy from stavudine to abacavir or zidovudine. *J. AIDS*, **38**, 263–267.
9. Caron,M., Auclair,M., Lagathu,C., Lombes,A., Walker,U.A., Kornprobst,M. and Capeau,J. (2004) The HIV-1 nucleoside reverse transcriptase inhibitors stavudine and zidovudine alter adipocyte functions in vitro. *AIDS*, **18**, 2127–2136.
10. Khosravi-Far,R. and Esposti,M. (2004) Death receptor signals to mitochondria. *Cancer Biol. Ther.*, **3**, 1051–1057.
11. Liu,X., Li,P., Widlak,P., Zou,H., Luo,X., Garrard,W.T. and Wang,X. (1998) The 40-kDa subunit of DNA fragmentation factor induces DNA fragmentation and chromatin condensation during apoptosis. *Proc. Natl Acad. Sci. USA*, **95**, 8461–8466.
12. Widlak,P., Li,P., Wang,X. and Garrard,W.T. (2000) Cleavage preferences of the apoptotic endonuclease DFF40 (caspase-activated DNase or nuclease) on naked DNA and chromatin substrates. *J. Biol. Chem.*, **275**, 8226–8232.
13. Enari,M., Sakahira,H., Yokoyama,H., Okawa,K., Iwamatsu,A. and Nagata,S. (1998) A caspase-activated DNase that degrades DNA during apoptosis, and its inhibitor ICAD. *Nature*, **391**, 43–50.
14. Compton,M.M. (1992) A biochemical hallmark of apoptosis: internucleosomal degradation of the genome. *Cancer Metastasis Rev.*, **11**, 105–119.
15. Wyllie,A.H., Morris,R.G., Smith,A.L. and Dunlop,D. (1984) Chromatin cleavage in apoptosis: association with condensed chromatin morphology and dependence on macromolecular synthesis. *J. Pathol.*, **142**, 67–77.
16. Bursch,W., Kleine,L. and Tenniswood,M. (1990) The biochemistry of cell death by apoptosis. *Biochem. Cell Biol.*, **68**, 1071–1074.
17. Staley,K., Blaschke,A.J. and Chun,J. (1997) Apoptotic DNA fragmentation is detected by a semi-quantitative ligation-mediated PCR of blunt DNA ends. *Cell Death Differ.*, **4**, 66–75.
18. Mueller,P.R. and Wold,B. (1989) In vivo footprinting of a muscle specific enhancer by ligation mediated PCR. *Science*, **246**, 780–786.
19. O'Doherty,U., Swiggard,W.J., Jeyakumar,D., McGain,D. and Malim,M.H. (2002) A sensitive, quantitative assay for human immunodeficiency virus type 1 integration. *J. Virol.*, **76**, 10942–10950.
20. Swiggard,W.J., Baytop,C., Yu,J.J., Dai,J., Li,C., Schretzenmair,R., Theodosopoulos,T. and O'Doherty,U. (2005) Human immunodeficiency virus type 1 can establish latent infection in resting CD4+ T cells in the absence of activating stimuli. *J. Virol.*, **79**, 14179–14188.
21. Saleh,S., Solomon,A., Wightman,F., Xhilaga,M., Cameron,P.U. and Lewin,S.R. (2007) CCR7 ligands CCL19 and CCL21 increase permissiveness of resting memory CD4+ T cells to HIV-1 infection: a novel model of HIV-1 latency. *Blood*, **110**, 4161–4164.
22. Zhang,L., Lewin,S.R., Markowitz,M., Lin,H.H., Skulsky,E., Karanicolas,R., He,Y., Jin,X., Tuttleton,S., Vesanen,M. *et al.* (1999) Measuring recent thymic emigrants in blood of normal and HIV-1-infected individuals before and after effective therapy. *J. Exp. Med.*, **190**, 725–732.
23. Reed,G.F., Lynn,F. and Meade,B.D. (2002) Use of coefficient of variation in assessing variability of quantitative assays. *Clin. Diagn. Lab Immunol.*, **9**, 1235–1239.
24. Ross,T.M. (2001) Using death to one's advantage: HIV modulation of apoptosis. *Leukemia*, **15**, 332–341.
25. Groux,H., Torpier,G., Monte,D., Mouton,Y., Capron,A. and Ameisen,J. (1992) Activation-induced death by apoptosis in CD4+ T cells from human immunodeficiency virus-lnfected asymptomatic individuals. *J. Exp. Med.*, **175**, 331–340.
26. Gougeon,M.L. and Piacentini,M. (2009) New insights on the role of apoptosis and autophagy in HIV pathogenesis. *Apoptosis*, **14**, 501–508.
27. Cherry,C., Skolasky,R., Lal,L., Creighton,J., Hauer,P., Raman,S., Moore,R., Carter,K., Thomas,D., Ebenezer,G. *et al.* (2006) Antiretroviral use and other risks for HIV-associated neuropathies in an international cohort. *Neurology*, **66**, 867–873.
28. Bohler,T., Walcher,J., Holzl-Wenig,G., Geiss,M., Buchholz,B., Linde,R. and Debatin,K.M. (1999) Early effects of antiretroviral combination therapy on activation, apoptosis and regeneration of T cells in HIV-1-infected children and adolescents. *AIDS*, **13**, 779–789.
29. Badley,A.D., Parato,K., Cameron,D.W., Kravcik,S., Phenix,B.N., Ashby,D., Kumar,A., Lynch,D.H., Tschopp,J. and Angel,J.B. (1999) Dynamic correlation of apoptosis and immune activation during treatment of HIV infection. *Cell Death Differ.*, **6**, 420–432.
30. Alnemri,E.S. and Litwack,G. (1990) Activation of internucleosomal DNA cleavage in human CEM lymphocytes by glucocorticoid and novobiocin. Evidence for a non-Ca2(+)-requiring mechanism(s). *J. Biol. Chem.*, **265**, 17323–17333.
31. Wang,H., Li,J., Bostock,R.M. and Gilchrist,D.G. (1996) Apoptosis: a functional paradigm for programmed plant cell death induced by a host-selective phytotoxin and invoked during development. *Plant Cell*, **8**, 375–391.
32. Gavrieli,Y., Sherman,Y. and Ben-Sasson,S. (1992) Identification of programmed cell death in situ via specific labeling of nuclear DNA fragmentation. *J. Cell Biol.*, **119**, 493–501.
33. Stepczynska,A., Lauber,K., Engels,I.H., Janssen,O., Kabelitz,D., Wesselborg,S. and Schulze-Osthoff,K. (2001) Staurosporine and conventional anticancer drugs induce overlapping, yet distinct pathways of apoptosis and caspase activation. *Oncogene*, **20**, 1193–1202.
34. Sordet,O., Liao,Z., Liu,H., Antony,S., Stevens,E.V., Kohlhagen,G., Fu,H. and Pommier,Y. (2004) Topoisomerase I-DNA complexes contribute to arsenic trioxide-induced apoptosis. *J. Biol. Chem.*, **279**, 33968–33975.
35. Lecoeur,H., Melki,M., Saïdi,H. and Gougeon,M. (2008) Analysis of apoptotic pathways by multiparametric flow cytometry: application to HIV infection. *Methods Enzymol.*, **442**, 51–82.
36. Li,X., Traganos,F., Melamed,M.R. and Darzynkiewicz,Z. (1995) Single-step procedure for labeling DNA strand breaks with fluorescein- or BODIPY-conjugated deoxynucleotides: detection of apoptosis and bromodeoxyuridine incorporation. *Cytometry*, **20**, 172–180.

37. Loo,D.T. (2002) TUNEL assay. An overview of techniques. *Methods Mol. Biol.*, **203**, 21–30.
38. Wright,D. and Manos,M. (1990) In: Innis,M., Gelfont,D., Sninsky,J. and White,T. (eds), *PCR Protocols: A Guide to Methods and Applications*. Academic Press, San Diego, pp. 153–158.
39. Schwartz,L.M. (1991) The role of cell death genes during development. *Bioessays*, **13**, 389–395.
40. Majno,G. and Joris,I. (1995) Apoptosis, oncosis, and necrosis. An overview of cell death. *Am. J. Pathol.*, **146**, 3–15.
41. Dal Canto,M.C. and Gurney,M.E. (1994) Development of central nervous system pathology in a murine transgenic model of human amyotrophic lateral sclerosis. *Am. J. Pathol.*, **145**, 1271–1279.
42. Sperandio,S., de Belle,I. and Bredesen,D.E. (2000) An alternative, nonapoptotic form of programmed cell death. *Proc. Natl Acad. Sci. USA*, **97**, 14376–14381.
43. Wyllie,A.H. and Golstein,P. (2001) More than one way to go. *Proc. Natl Acad. Sci. USA*, **98**, 11–13.